$Ce_{2/3}Cr_{1/3}O_{2+y}$: A New Oxygen Storage Material Based on the Fluorite Structure

Preetam Singh, M. S. Hegde, and J. Gopalakrishnan*

Solid State and Structural Chemistry Unit, Indian Institute of Science, Bangalore 560012, India

Received August 15, 2008. Revised Manuscript Received October 10, 2008

In an exploratory search for new oxygen storage materials (OSMs), we have identified a fluorite-type solid solution series, $Ce_{1-x}Cr_xO_{2+y}$ ($0 < x \leq 1/3$), of which the $x = 1/3$ member, $Ce_{2/3}Cr_{1/3}O_{2.11}$ (oxide **I**), exhibits excellent reversible oxygen release/storage properties at relatively low temperatures (~350 °C). Oxide **I** prepared by a hydrothermal route crystallizes in a metastable nanocrystalline (~4 nm) fluorite type structure ($a = 5.352$ Å) where the cerium and chromium are randomly distributed. Characterization of oxide **I** by electron microscopy, powder X-ray diffraction, X-ray photoelectron spectroscopy, and thermogravimetry for the composition, crystal structure, oxidation states of metal atoms, and oxygen stoichiometry yields the formula $Ce^{IV}{}_{2/3}Cr^{VI}{}_{1/9}Cr^{IV}{}_{2/9}O_{2.10 \pm 0.02}$ for oxide **I**. Investigation of oxygen release/intake by temperature programmed hydrogen reduction and thermogravimetric studies has revealed that oxide **I** possesses a high oxygen storage capacity of 0.175 moles of O_2/mole up to 550 °C; this value is better than or comparable to the best OSMs based on CeO_2-ZrO_2. The temperature (~350 °C) at which facile oxygen release/intake occurs with oxide **I** is also lower than that of CeO_2-ZrO_2 based oxides. Formation of oxide **I** with a cation-disordered fluorite structure, unlike other lanthanide analogs, and its oxygen release/storage properties are discussed in terms of the redox chemistry of $Ce^{IV/III}$ and $Cr^{VI/IV}$ in the solid state.

Introduction

Solid materials that store and release oxygen reversibly at moderate temperatures (oxygen storage materials ≡ OSMs) have proven/potential application in many fields of technology. CeO_2-ZrO_2 mixed oxides are well-known OSMs that already find application as three-way catalyst for the removal of NO_x, CO, and hydrocarbons from automobile exhaust emissions.[1,2] Other applications envisaged for OSMs include: improving the efficiency of H_2-O_2 fuel cells by incorporating them in the cathode,[3] hydrocarbon/soot oxidation catalysts for emission control from diesel engines[4] and possibly for the production of hydrogen by thermochemical water splitting.[5] To meet these demands, there is a need for new OSMs that store and release large quantities of oxygen at relatively low temperatures (<400 °C). Rare earth oxysulfates, $R_2O_2SO_4$ (R = rare earth), are a new class of OSMs[6−8] due to the reaction $R_2O_2SO_4 \rightarrow R_2O_2S + 2O_2$ that occurs at relatively higher temperatures (≥700 °C). Our efforts to understand and develop new/better OSMs have revealed[9] a synergistic redox role between Ce/Zr that renders CeO_2-ZrO_2 oxides better OSMs than the corresponding CeO_2-HfO_2 oxides. Continuing our efforts in this direction with several CeO_2-MO_x (M = transition metal) systems and keeping in view the Ce/M redox characteristics in oxides as well as crystal chemistry, we have been able to develop a new OSM based on CeO_2-CrO_3 oxides. The new material, synthesized by a soft-chemical hydrothermal route and stabilized in the fluorite structure through a $Ce^{IV/III}-Cr^{VI/IV}$ redox process, exhibits excellent oxygen storage/release property that appears to be better than or at least competitive to that of the CeO_2-ZrO_2-based oxides. The details of synthesis, structure and investigation of oxygen storage/release behavior of the best composition in the CeO_2-CrO_3 system, viz., $Ce_{2/3}Cr_{1/3}O_{2+y}$, are described in this paper. After we have completed our work, we came across the report[10] of a new series of oxygen storage materials, $REBaCo_4O_{7+\delta}$ (RE = rare earth), that show a similar oxygen storage capacity.

Experimental Section

CeO_2-CrO_3 mixed oxides were synthesized by a hydrothermal method from the starting materials, $(NH_4)_2Ce(NO_3)_6$ (CAN), CrO_3, and diethylenetriamine (DETA), taken in the molar ratio $(1-x)$, x,

* Corresponding author. E-mail: gopal@sscu.iisc.ernet.in. Phone: 91-80-2293 2537. Fax: 91-80-2360 1310.

(1) Trovarelli,A. In *Catalysis by Ceria and Related Materials*; Hutchings, G. J. , Ed.; Catalytic Science Series; Imperial College Press: London, 2002; Vol. 2.
(2) Di Monte, R.; Kašpar, J. *J. Mater. Chem.* **2005**, *15*, 633.
(3) Xu, Z.; Qi, Z.; Kaufman, A. *J. Power Sources.* **2003**, *115*, 40.
(4) Machida, M.; Murata, Y.; Kishikawa, K.; Zhang, D.; Ikeue, K. *Chem. Mater.* **2008**, *20*, 4489.
(5) Kodama, T.; Gokon, N. *Chem. Rev.* **2007**, *107*, 4048.
(6) Machida, M.; Kowamura, K.; Ito, K. *Chem. Commun.* **2004**, 662.
(7) Machida, M.; Kowamura, K.; Ito, K.; Ikeue, K. *Chem. Mater.* **2005**, *17*, 1487.
(8) Machida, M.; Kawano, T.; Eto, M.; Zhang, D.; Ikeue, K. *Chem. Mater.* **2007**, *19*, 954.
(9) Baidya, T.; Hegde, M. S.; Gopalakrishnan, J. *J. Phys. Chem. B* **2007**, *111*, 5149.
(10) (a) Karppinen, M.; Yamauchi, H.; Otani, S.; Fujita, T.; Motohashi, T.; Huang, Y. H.; Valkeapää, M.; Fjellvag, H. *Chem. Mater.* **2006**, *18*, 490. (b) Motohashi, T.; Kadota, S.; Fjellvag, H.; Karppinen, M.; Yamauchi, H. *Mater. Sci. Eng., B* **2008**, *148*, 196. (c) Kadota, S.; Karppinen, M.; Motohashi, T.; Yamauchi, H. *Chem. Mater.* **2008**, *20*, 6378.

10.1021/cm802207a CCC: $40.75 © 2008 American Chemical Society
Published on Web 11/11/2008

and 3.00, respectively. Typically, for the synthesis of $Ce_{2/3}Cr_{1/3}O_{2+y}$ ($x = 1/3$), 6.67 mmol of CAN were dissolved in 20 mL of distilled water and 3.33 mmol of CrO_3 were dissolved in 15 mL of distilled water. Both the solutions were mixed and 0.03 moles (3.1 mL) of DETA were added. The resulting mixture turned into a dark yellow colored gel. The volume of the gel was made up to 45 mL with water and transferred to three Teflon-lined hydrothermal pressure vessels (of 20 mL capacity) and tightly closed. The pressure vessels were heated at 200 °C for 24 h in a hot air oven. After the reaction, the solid products were centrifuged out, washed and dried at 110 °C. $x = 0.10$ and 0.20 members of the $Ce_{1-x}Cr_xO_{2+y}$ series were synthesized by a similar procedure by reacting appropriate amounts of CAN, CrO_3, and DETA.

Characterization of the solid products was carried out by scanning electron microscopy (SEM) and energy-dispersive X-ray (EDX) analysis (JEOL JSM - 5600LV Scanning Electron Microscope) and powder X-ray diffraction (XRD) (Philips X'Pert Diffractometer fitted with graphite crystal monochromator, Cu Kα radiation). Structures were refined by the Rietveld method on the CeO_2-fluorite model by means of Fullprof program.[11] For this purpose, XRD data were collected at a scan rate of 0.25° 2θ min^{-1} with a 0.01° step size in the 2θ range between 10 and 80°. For Transmission electron microscopy (TEM) studies, a toluene dispersion of the sample was dropped onto holey carbon coated Cu grids and the images were recorded with FeI Technai 20 instrument at 200kV. X-ray photoelectron spectra (XPS) were recorded on a Thermoscientific Multilab 2000 equipment employing Al Kα X-rays. XPS binding energies are accurate within ± 0.1 eV. Thermogravimetric (TG) analyses were carried out on a home-built apparatus in flowing 10% H_2/Ar (30 mL/min) and in air in the temperature range 30−600 °C at a heating rate of 4 °C/min.

Oxygen storage/release properties of $Ce_{1-x}Cr_xO_{2+y}$ were studied by hydrogen intake measurements carried out in a microreactor (30 cm length and 0.4 cm internal diameter) employing 5.49% H_2/Ar (certified calibration gases mixture obtained from Bhoruka Gases Ltd., Bangalore, India) with 30 sccm flow rate and 10 °C/min heating rate, up to 550 °C. Volume of hydrogen intake/consumption by the sample was calibrated against CuO standard. CO oxidation and direct O_2 evolution from the $Ce_{1-x}Cr_xO_{2+y}$ samples were investigated in a similar microreactor employing 1 vol % CO/He and UHP He gases, respectively, at a total gas flow of 100 sccm over 250 mg of oxide sample at a linear heating rate of 10 °C min^{-1} up to 600 °C. Gaseous products were analyzed by means of a quadrupole mass spectrometer.

Results and Discussion

We investigated the formation of fluorite-type phases in CeO_2-MO_x for several transition metals such as M = Ti, V, Cr, Mn, Fe, and Ru, employing hydrothermal synthesis method (described in the Experimental Section). Fluorite-type phases were formed for M = Ti, Cr, Mn, Fe, and Ru over different ranges of composition. Subsequent investigations revealed that clean reproducible characteristics in terms of phase stability and reversible oxygen release and intake were displayed by members of $Ce_{1-x}Cr_xO_{2+y}$ system, of which the composition with $x = 1/3$, $Ce_{2/3}Cr_{1/3}O_{2+y}$ (**I**) turned out to be the best OSM. Therefore, we largely focus our results and discussion on this particular composition. In doing so, we recognize the toxicity of chromium, especially Cr(VI), and related concerns for the actual use of these materials in application/technology and therefore we do not suggest that these materials could serve as a replacement straightaway for the existing Ce−Zr−O oxides.

Oxide **I** obtained by the hydrothermal route is single phase fluorite with $a = 5.352$ (2) Å (Figure 1a and Table 1). SEM and EDX data further confirm single phase nature of this material with 2:1 Ce/Cr stoichiometry (Ce = 0.65 ± 0.02 and Cr = 0.35 ± 0.02). It should be mentioned that, for $Ce_{1-x}Cr_xO_{2+y}$ samples, the nominal composition and the final composition remain the same for $x \leq 1/3$. TEM images and corresponding electron diffraction (ED) patterns (Figure 2) of $x = 1/3$ composition (oxide **I**) show that the as-prepared and dried sample is nanocrystalline in nature, having crystallites in the range of ∼ 4 nm in size. Line widths of powder XRD reflections (Figure 1a) are consistent with the nanocrystalline particle sizes (average particle size estimated from line width is ∼ 4 nm).

We investigated the oxidation states of chromium and cerium in **I** by means of XPS. Core level Cr (2p) spectrum for oxide **I** is compared with the corresponding spectra for Cr_2O_3 and CrO_3 in Figure 3. The data clearly reveal that, contrary to our expectation of $Ce_2^{III}Cr^{VI}O_6$ formulation for oxide **I**, chromium occurs in a mixed-valence state with the likely oxidation states of Cr^{IV} and Cr^{VI} roughly in the ratio 2:1. Cr ($2p_{3/2}$) binding energies (BE) for these two states obtained from the spectrum (Figure 3a), 576.9 and 579.3 eV, are consistent with the expected BE values for Cr (IV) and Cr (VI) in oxides.[12] The Ce 3d XPS spectrum (Figure 4a) shows that cerium occurs in the IV state in oxide **I** (Ce $3d_{5/2}$ BE in oxide **I** is 881.8 and 881.7 eV in CeO_2). Independent estimate of oxygen stoichiometry, obtained by iodometric titration, gave the value, $Ce_{2/3}Cr_{1/3}O_{2.10\pm0.02}$. Combining this result with XPS results, we formulate oxide **I** as $Ce^{IV}{}_{2/3}Cr^{VI}{}_{1/9}Cr^{IV}{}_{2/9}O_{2.11}$.

Thermogravimetry (TG) (Figure 5) not only provides additional support to the above formula but also reveals the nature of oxygen release/intake by this material. The total weight loss under reducing condition (Figure 5a) up to 700 °C (stage 3) is 6.8%. The weight loss calculated for the reduction reaction

$$Ce^{IV}_{2/3}Cr^{VI}_{1/9}Cr^{VI}_{2/9}O_{2.11} + 0.61H_2 \rightarrow Ce^{III}_{2/3}Cr^{III}_{1/3}O_{1.5} + 0.61H_2O \quad (1)$$

is 6.75%. We see a change in slope around 275 °C (stage 1) and a small plateau around 600 °C (stage 2) in the TG curve (Figure 5a). The weight loss found up to 275 °C is ∼2.5%,which is close to the weight loss expected for the reaction (2.8%)

$$Ce^{IV}_{2/3}Cr^{VI}_{1/9}Cr^{VI}_{2/9}O_{2.11} + 0.275H_2 \rightarrow Ce^{IV}_{2/3}Cr^{III}_{1/3}O_{1.835} + 0.275H_2O \quad (2)$$

The weight loss found up to 600 °C (stage 2) is ∼ 6.0%, which would correspond to the composition $Ce^{IV}{}_{0.147}$-$Ce^{III}{}_{0.52}Cr^{III}{}_{0.333}O_{1.573}$. We have checked the powder XRD patterns of the sample obtained at all the three stages 1, 2

(11) Rodriguez-Carvajal, J. *Multipattern Rietveld Refinement Program FullProf 2k*, version 3.30; Laboratiore Léon Brillouin, CEA: Saclay, France, 2005.

(12) Ikemoto, I.; Ishii, K.; Kinoshita, S.; Kuroda, H.; Alario Franco, M. A.; Thomas, J. M. *J. Solid State Chem.* **1976**, *17*, 425.

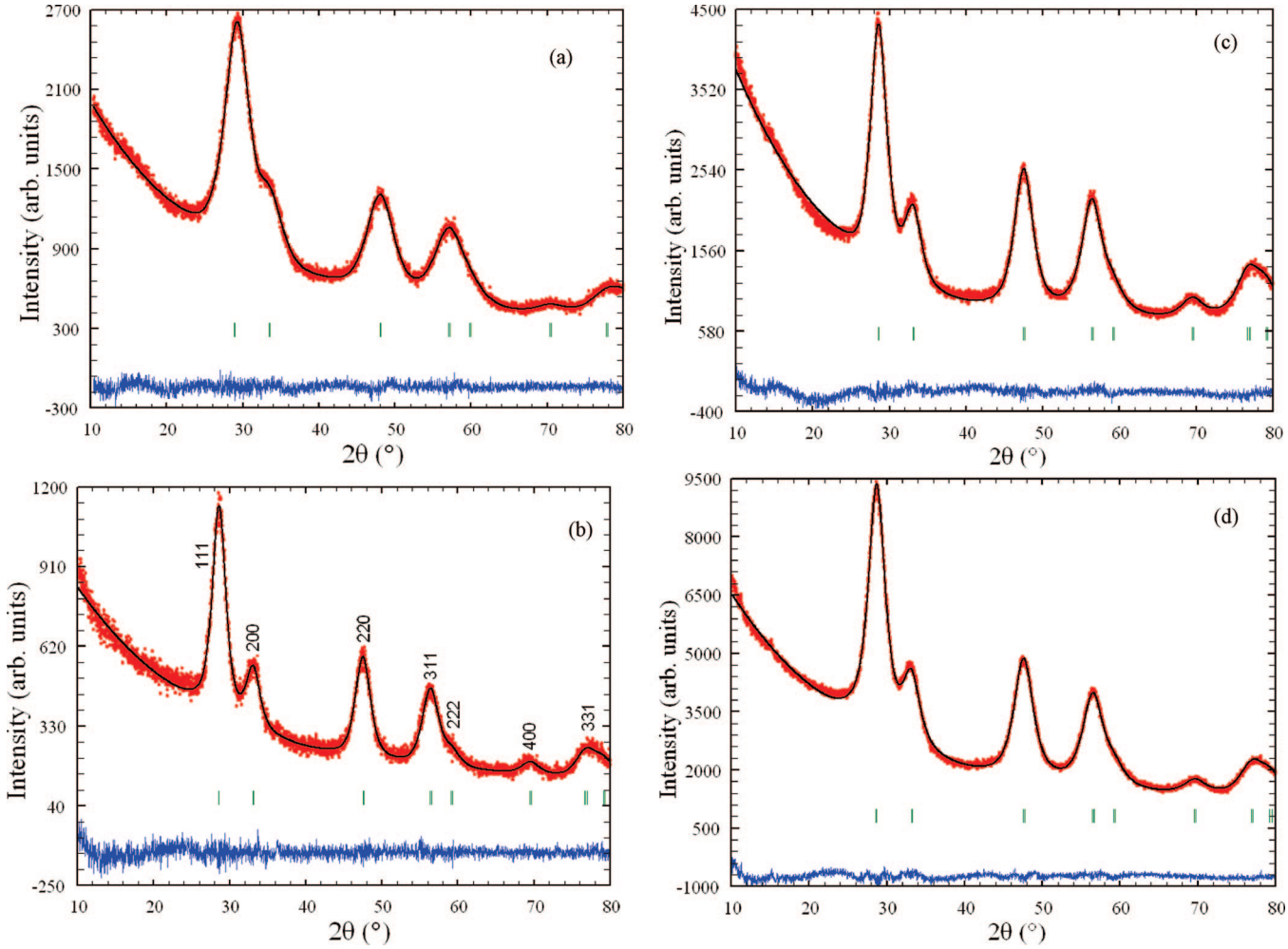

Figure 1. Rietveld refined powder XRD profiles of (a) oxide **I**, $Ce_{2/3}Cr_{1/3}O_{2.10\pm0.02}$; (b) oxide **I** reduced in hydrogen/argon up to 550 °C, $Ce_{2/3}Cr_{1/3}O_{1.60\pm0.02}$; (c) oxide **I** heated in air up to 550 °C, $Ce_{2/3}Cr_{1/3}O_{1.84\pm0.02}$; (d) sample (b) and (c) reoxidized in air, $Ce_{0.667}Cr_{0.333}O_{2.10\pm0.02}$. The vertical bars show the *hkl* reflections corresponding to the fluorite structure. The difference profile is shown at the bottom.

Table 1. Structural Characterization of Oxide I and Its Derivatives

s. no.	composition	description	lattice param a (Å)	R_B[a]	R_f[b]	average crystallite sizes from XRD (TEM) (nm)
1	$Ce_{2/3}Cr_{1/3}O_{2.1\pm0.02}$ (oxide **I**)	as prepared, dried at 110 °C	5.352 (2)	0.39	0.30	3.0 (4 ± 1)
2	$Ce_{2/3}Cr_{1/3}O_{1.84\pm0.02}$	oxide **I** heated in air up to 550 °C	5.367 (3)	1.42	0.70	4.0
3	$Ce_{2/3}Cr_{1/3}O_{1.60\pm0.02}$	oxide **I** reduced in H_2/Ar up to 550 °C	5.407 (2)	1.29	0.86	4.0
4	$Ce_{2/3}Cr_{1/3}O_{2.1\pm0.02}$	oxide (3) reoxidized in air at 110 °C	5.374 (2)	1.21	0.79	4.0
5	$Ce_{0.90}Cr_{0.10}O_{2.05}$	as prepared, dried at 110 °C	5.396 (1)	1.29	0.89	4.5
6	$Ce_{0.80}Cr_{0.20}O_{2.05}$	as prepared, dried at 110 °C	5.382 (2)	1.16	0.74	3.0 (4 ± 1)
7	CeO_2	as prepared, dried at 110 °C	5.415 (1)	3.12	2.38	12.0 (12 ± 1)

[a] Reliability factors for profile refinement. [b] Reliability factors for profile refinement.

and 3. The completely reduced product (stage 3) was found to be a mixture of perovskite like $CeCrO_3$ ($a \simeq 3.87$Å) and fluorite like CeO_{2-y} ($a \simeq 5.425$Å). Intermediate products 1 and 2 however retain the fluorite structure. We show the Rietveld refined powder XRD pattern of the product obtained by heating oxide **I** up to 550 °C in H_2/Ar in Figure 1b (Table 1, $a = 5.407$ (2) Å). The Cr (2p) and Ce (3d) XPS spectra (Figure 3 b and 4b) show that Cr is in the III state and cerium in mixed (III/IV) state in this product, as expected from TG weight loss data.

Oxide **I** releases oxygen in air itself as revealed by TG (Figure 5b) and the weight loss found up to 550 °C is ~2.8%. The product at this stage retains the fluorite structure (Figure 1c). Interestingly, the reduced fluorite-type products obtained both in hydrogen and air could be reoxidized by heating in oxygen/air almost regaining the weight corresponding to the starting material, oxide **I** (Figure 5c). Accordingly, we see that oxide I could function as a reversible OSM within the temperature range of 550 °C; oxygen release starts at as low a temperature as 250 °C in hydrogen and at 400 °C in air.

Oxygen release/storage properties of $Ce_{1-x}Cr_xO_{2+y}$ oxides were investigated by temperature programmed hydrogen reduction (TPR) studies (Figure 6). Oxide **I** takes up hydrogen from 250 °C and reduction is complete around ~350 °C (peak in Figure 6a). Total oxygen release estimated from the area under the curve (Figure 6a) corresponds to about 0.36 O which is equivalent to about 4% weight loss; the latter is consistent with the TG weight

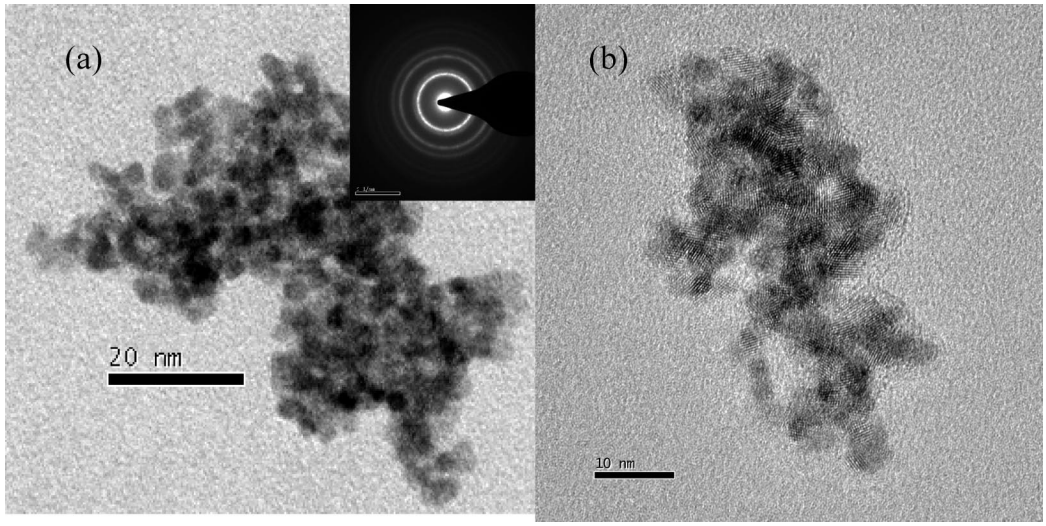

Figure 2. (a) TEM image of oxide **I** (bright field). The corresponding ED pattern is shown in inset. (b) HRTEM image of oxide **I** showing nanocrystalline nature of the sample.

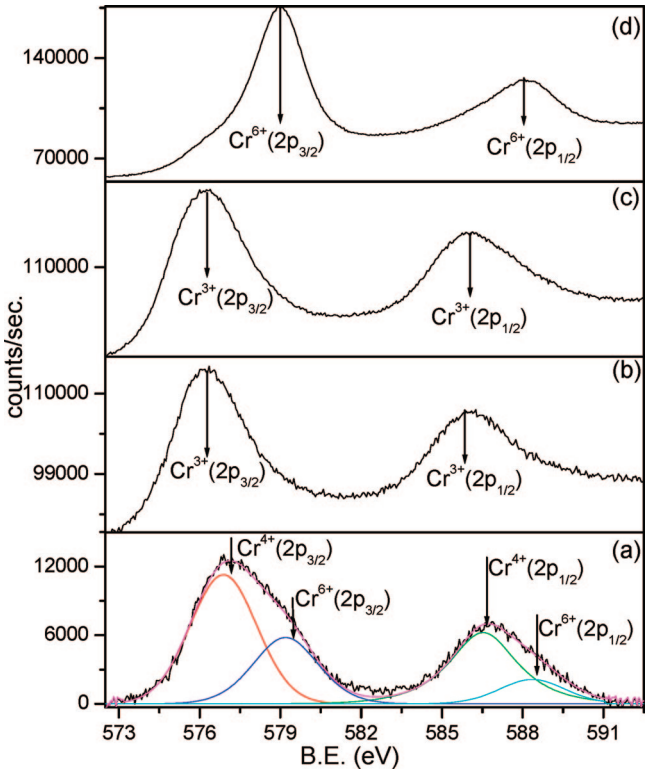

Figure 3. Cr (2p) core level XPS of (a) oxide **I**, and (b) oxide **I** reduced in hydrogen/argon up to 550 °C. For comparison, the corresponding spectra of (c) Cr_2O_3 and (d) CrO_3 are shown.

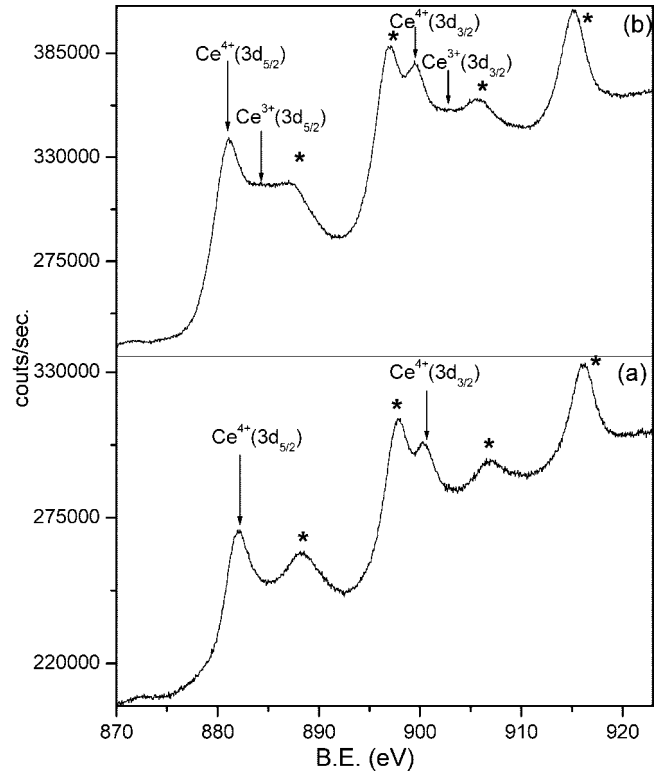

Figure 4. Ce (3d) XPS spectra of (a) oxide **I** and (b) oxide **I** reduced in hydrogen/argon up to 550 °C. Asterisks (*) indicate corresponding satellite peaks for Ce^{4+} state.

loss (eq 2). $Ce_{1-x}Cr_xO_{2+y}$ oxides with $x = 0.1$ and $x = 0.2$ also show hydrogen intake at slightly higher temperatures with smaller amount of oxygen release (lines b and c in Figure 6) that is consistent with the composition. For comparison, we also show the hydrogen intake curves for fluorite $Ce_{0.5}Zr_{0.5}O_2$ and CeO_2 under similar conditions in Figure 6d and e respectively. In Figure 7, we show TPR curves for five cycles and the data for a sample stored for a long time (6 months), revealing that the oxygen release/storage property of oxide **I** is robust with respect to cycling up to ~550 °C and "aging".

Clearly, hydrogen intake/oxygen release from oxide **I** occurs at a lower temperature than from $Ce_{0.5}Zr_{0.5}O_2$. Also, pure CeO_2 does not show a significant hydrogen intake in this temperature range. Thus, hydrogen intake studies establish that oxide **I** is a better OSM than $Ce_{0.5}Zr_{0.5}O_2$. It should be mentioned that the reduced/decomposed sample obtained by heating the oxide **I** in hydrogen/argon (containing $CeCrO_3$ and CeO_{2-y}) shows a much less oxygen storage capacity (~0.07 moles O_2/mole).

Interestingly, oxide **I** releases oxygen even under nonreducing conditions. A TPR study of the gaseous products evolved when oxide **I** is heated in a flow of He gas (Figure

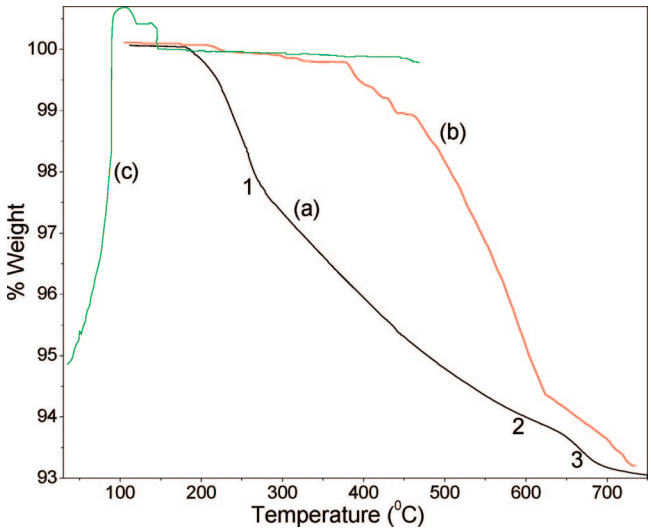

Figure 5. Thermogravimetry (TG) curves for (a) reduction of oxide **I** in hydrogen/argon, (b) reduction of oxide **I** in air, and (c) reoxidation of oxide **I** reduced in hydrogen/argon up to 555 °C.

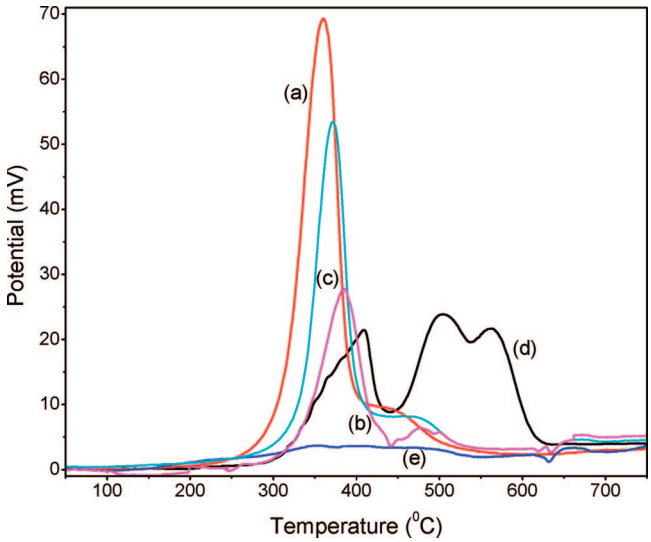

Figure 6. (a) Temperature-programmed H_2 consumption/intake for the reduction of oxide **I**. The corresponding data for $x = 0.1$ and $x = 0.2$ members of $Ce_{1-x}Cr_xO_{2+y}$ are shown in (b) and (c), respectively. For comparison, the data for (d) $Ce_{0.5}Zr_{0.5}O_2$ and (e) CeO_2 are also shown.

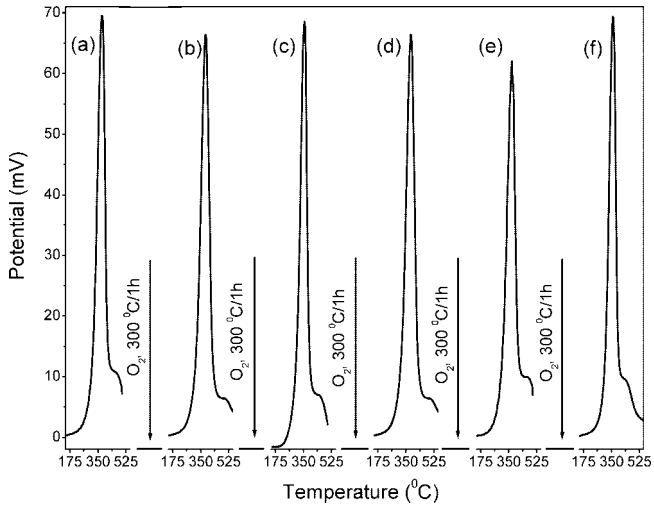

Figure 7. Temperature-programmed hydrogen consumption/intake for the reduction of oxide **I** showing reversible reduction/oxidation for five cycles (a−e). Curve (f) was recorded on a sample of oxide I stored for about 6 months, showing no significant deterioration of oxygen storage capacity.

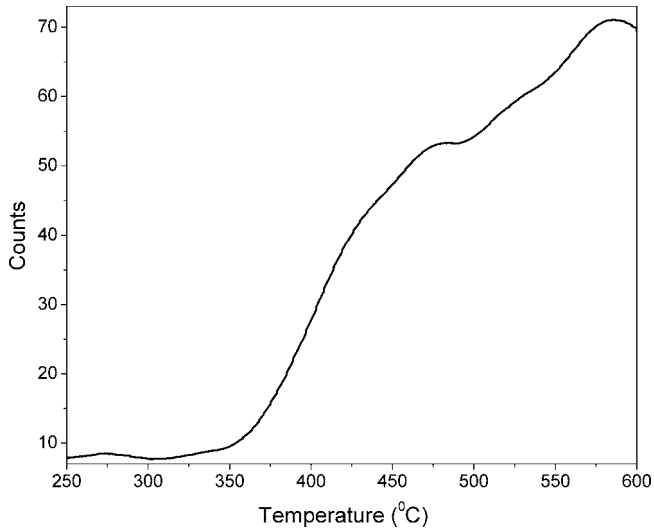

Figure 8. Temperature-programmed oxygen release from oxide **I** when heated in He flow, recorded by a quadrupole mass spectrometer.

8) shows that oxygen release occurs at ∼350 °C. We have also investigated CO oxidation over oxide **I** under anaerobic conditions (absence of external oxygen gas). From Figure 9a, we see that CO oxidation starts at as low a temperature as ∼200 °C. Under similar conditions, CO oxidation over $Ce_{0.5}Zr_{0.5}O_2$ occurs >300 °C (Figure 9b).

Our results described above show that oxide **I** is a better OSM than $Ce_{1-x}Zr_xO_2$ oxides, both in terms of total oxygen storage capacity and the temperature range at which oxygen release/intake occurs. The maximum oxygen storage capacity expected for $Ce_{0.5}Zr_{0.5}O_2$ is 0.125 moles of O_2/mole (1693 μM/g) and the experimentally observed value up to 500 °C for one of the best $Ce_{0.5}Zr_{0.5}O_2$ samples is 0.11 moles of O_2/mole (1500 μM /g).[13] For oxide **I**, the corresponding values are (0.18 moles of O_2/mole; 2603 μM /g: expected) and (0.175 moles of O_2/mole; 2513 μM/g: found up to 550 °C). It is known[13] that highest oxygen storage capacity is obtained for disordered/atomically homogeneous CeO_2-ZrO_2 oxides with the fluorite structure. We believe that formation of oxide **I** with the fluorite structure where Ce/Cr are atomically disordered is one of the factors that contributes to a high oxygen storage capacity. Another likely factor that favors the high oxygen storage capacity is that, whereas $Ce_{0.5}Zr_{0.5}O_2$ depends on Ce^{IV}/Ce^{III} redox couple for its oxygen storage/release, oxide **I** employs both Ce^{IV}/Ce^{III} and $Cr^{VI/IV}/Cr^{III}$ redox processes for its oxygen storage/release.

Formation of oxide **I** with a fluorite structure where cerium and chromium are disordered stands in contrast to the well-defined layered structure of other lanthanide oxychromates, $Ln_2O_2CrO_4$ (Ln = rare earth).[14] This difference in structure most likely arises from the redox characteristics of $Ce^{IV}/$

(13) Nagai, Y.; Yamamoto, T.; Tanaka, T.; Yoshida, S.; Nonaka, T.; Okamoto, T.; Suda, A.; Sugiura, M. *Catal. Today* **2002**, *74*, 225.

(14) Charkin, D. O.; Grischenko, R. O.; Sadybekov, A. A.; Goff, R. J.; Lightfoot, P. *Inorg. Chem.* **2008**, *47*, 3065.

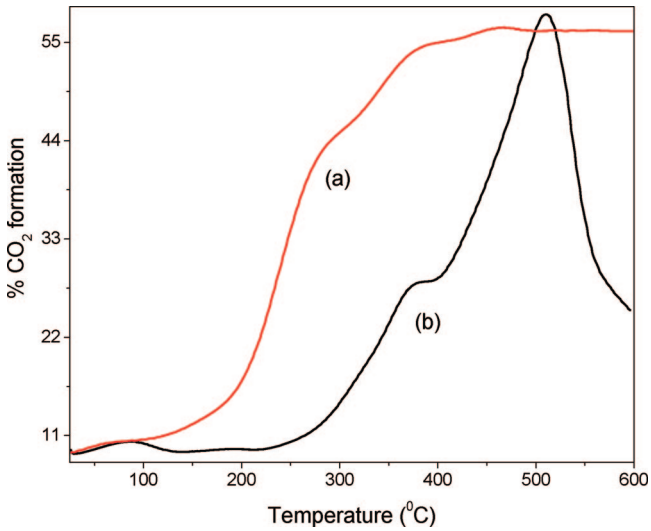

Figure 9. (a) Anaerobic oxidation of CO by oxide **I**. For comparison, data for CO oxidation over $Ce_{0.50}Zr_{0.50}O_2$ are shown in (b).

Ce^{III} (1.61 eV) and Cr^{VI}/Cr^{III} (1.33 eV).[15] In aqueous media, one would therefore expect from the solution redox potentials that the equilibrium

$$3Ce^{IV} + Cr^{III} \leftrightarrow 3Ce^{III} + Cr^{VI} \quad (3)$$

would lie to the right. Accordingly, the ideal formulation of $Ce_{2/3}Cr_{1/3}O_2$ would be $Ce^{III}{}_2Cr^{VI}O_6$, similar to other lanthanide analogs.[14] On the contrary, formation of oxide **I** with the cation disordered fluorite structure where chromium is in a mixed-valence (Cr^{IV}/Cr^{VI}) state and cerium is almost exclusively in the IV state could be due to the redox instability of Cr^{VI} in the fluorite structure, where it would be coordinated to eight oxygen atoms.[16] Cr^{VI}, which is normally stabilized in the tetrahedral oxygen coordination ($CrO_4{}^{2-}$), would be highly unstable in the fluorite structure, bringing down the empty Cr^{VI}:$3d^0$ closer to O (2p) states and closer to CeIII/Ce^{IV} redox energy[16] (Figure 10). Accordingly, an electron transfer from Ce^{III} to Cr^{VI} becomes facile in the solid state. Thus $Ce_{2/3}Cr_{1/3}O_2$ fluorite would be $Ce^{IV}{}_2Cr^{IV}O_6$ rather than $Ce^{III}{}_2Cr^{VI}O_6$ in the solid state. Presumably, further oxidation of $Ce^{IV}{}_2Cr^{IV}O_6$ occurs under our synthesis conditions to yield the actual oxide **I** with the formula $Ce^{IV}{}_2Cr^{VI}{}_{1/3}Cr^{IV}{}_{2/3}O_{6.3}$, where chromium exists in a mixed-valence (Cr^{VI}/Cr^{IV}) state. Structurally, excess oxygens could be accommodated at interstitial sites in the fluorite structure.[17]

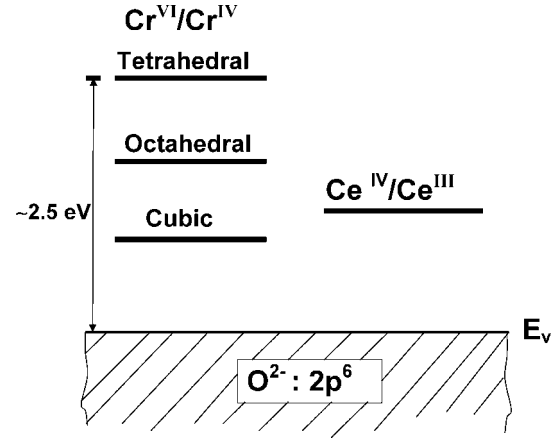

Figure 10. Schematic redox energies of Cr^{VI}/Cr^{IV} in tetrahedral, octahedral and cubic (8) oxygen coordination relative to Ce^{IV}/Ce^{I} redox energy (after ref 16).

In summary, we have described a new metastable fluorite-type oxide of the composition, $Ce_{2/3}Cr_{1/3}O_{2.11}$ (a = 5.352 (2) Å), where Ce^{IV} and mixed valent Cr^{VI}/Cr^{IV} are randomly distributed at the cation sites of the fluorite structure. The material exhibits a high oxygen storage capacity of 0.175 moles O_2/mole up to 550 °C (retaining the fluorite structure) and a facile oxygen release/intake at a relatively low temperature of ~350 °C under reducing conditions. Moreover, the material also releases oxygen under anaerobic condition around 350 °C and oxidizes CO at ~200 °C. All these characteristics make the oxide **I** an excellent OSM that is better than or at least competitive to $Ce_{1-x}Zr_xO_2$ oxides. Further investigations to show the viability of $Ce_{1-x}Cr_xO_{2+y}$ oxides for catalytic and other applications should keep in mind the toxicity of chromium(VI).

Acknowledgment. Financial support for this study from the Department of Science and Technology (DST), Government of India, is gratefully acknowledged. J.G. thanks the DST for the award of a Ramanna fellowship. Thanks are also due to Mr. R. M. Tiwari for help with TG studies.

CM802207A

(15) Cotton, F. A.; Wilkinson, G. *Advanced Inorganic Chemistry*, 3rd ed.; Wiley Eastern: New Delhi, India, 1972; pp 8411072.
(16) Goodenough, J. B. In *Chemistry and Uses of Molybdenum*; Barry, H. F., Mitchell, P.C. H. , Eds.; Climax Molybdenum Co.: Ann Arbor, MI, 1982; pp 1−22.
(17) Rao, C. N. R.; Gopalakrishnan, J. *New Directions in Solid State Chemistry*; Cambridge University Press: Cambridge, U.K., 1997; pp 255−257.